SPEA-E552 - Environmental Engineering

Comparison of Buffer Strips and Constructed Wetland Sizing for Removal of Aquatic NO_3 Pollution

Andrew J. Brown
Instructor: **Garth Linder**
December 9, 2021

Abstract

Nutrient pollution is a severe, chronic problem in North American agricultural waterways. Two important interventions, constructed wetlands and buffer strips, have the potential to improve water quality and provide other important cobenefits to the surrounding landscape. However, sizing of these facilities is important to evaluate, as larger sizing drives cost and complexity. A constructed wetland and a series of buffer strips were evaluated using mass balance and a first-order plug flow reactor model to determine which intervention was more space-efficient for the Driftwood watershed in southeastern Indiana. The constructed wetland as modeled required 3731 acres of space to process nitrates at design flow, concentration, and temperature, while a series of buffer strips required 90000 acres. From a space-efficiency perspective, the constructed wetland is therefore favorable. However, additional investigation of a combined approach is recommended as a means of improving within-watershed stream habitat and water quality. Additional model development is also recommended to reach more nuanced and confident conclusions.

Contents

List of Figures

1 Introduction

1.1 background

Agricultural non-point source pollution is a persistent and expanding water quality problem in the Midwestern United States. Non-point source pollution causes biodiversity loss and the exacerbation of the freshwater biodiversity crisis (Dudgeon et al. 2006; Doering et al. 1999). Persistent eutrophication and pathogenic pollution directly destroy the recreational value of waterways (Doering et al. 1999; Keiser and Shapiro 2018; Segerson and Walker 2002), damage their habitat diversity (Bradshaw et al. 2020; Dahl 1990; Blann et al. 2009), and threaten public health (Ward et al. 2018). Abating these consequences is therefore imperative for improving environmental quality.

Constructed wetland and riparian buffer strips are especially interesting as tools to reduce agricultural pollution. Constructed wetlands provide many co-benefits, including nutrient abatement (Kovacic et al. 2000), additional habitat for threatened species (Bradshaw et al. 2020), and flood mitigation (Dahl 1990; Hey and Philippi 1995; Blann et al. 2009; Wine and Davison 2019). Buffer strips are similarly attractive tools for their improvement of biodiversity, nutrient retention, and hydrologic parameters (Stutter, Chardon, and Kronvang 2012; Mander and Tournebize 2015; Anbumozhi, Radhakrishnan, and Yamaji 2005). However, there is ambiguity around the benefits of wetlands and riparian buffers on larger scales (Doering et al. 1999; Evenson et al. 2021; Hansen et al. 2015; Kousky et al. 2013; Land et al. 2016; Stutter, Chardon, and Kronvang 2012). Ultimately, however, both approaches show enough promise at local scale to merit first order evaluation of feasibility as watershed interventions (Kovacic et al. 2000; Yang and Best 2015; Stutter, Chardon, and Kronvang 2012).

1.2 Goal & Scope

The goal of this analysis is to perform a first-order approximation of the sizing of a constructed free water surface wetland and a riparian buffer strip for the abatement of nitrogen pollution in the form of NO_3^- in the Driftwood Watershed, SE Indiana, from a mass-balance basis. Extensions for both interventions suggest some of the complexity underlying base assumptions and illustrate parts of the analysis necessary for a full evaluation of their feasibility. Economic and logistical issues are not considered, despite being very important parts of the evaluation process for both forms of intervention (Crites, Middlebrooks, and Reed 2006; Kadlec and Knight 1996; Hammer 1989; Reed, Middlebrooks, and Crites 1988). A discussion of the limitations of the analysis, with implications for likely differences in behavior from that modeled, is found in section 3. One watershed is analyzed to illustrate the first-approximation procedures for one case, with the expectation that these procedures could be potentially formalized and generalized in the future for analysis of multiple watersheds and further extension. Only NO_3^- is considered due to the complexities of modeling multiple nutrient and biochemical pollution inputs from non-point sources, and to limit the complexity of modeling multiple forms and transformations of single pollutants (Crites, Middlebrooks, and Reed 2006; Kadlec and Knight 1996; Shortle and Horan 2017).

2 Evaluation

Each intervention strategy was evaluated using a mass balance approach. Additional details were included only as relevant for an expedient, first-order approximation of the problem, and should not be construed as a complete design. Each evaluation's critical assumptions are described to illustrate other important factors held constant or neglected in the present analysis.

2.1 Design Watershed

The design watershed for the study is the Driftwood Watershed. The driftwood watershed has an area of 1165 mi^2 (3017 km^2) . The watershed's land use is predominantly agricultural, with 27% corn and 32% soybeans by area, respectively. Smaller land uses include several small municipalities and a small section of forest in the southwestern corner of the watershed. Figure 1 shows a map of the watershed and corn & soy extent. Figure 2 shows the watershed's waterways and USGS monitoring stations. The southernmost USGS gauging station was used to calibrate the scale of flows for the wetland project evaluation. Data were sourced from the USGS and the USDA (USGS 2019; USDA 2021; USGS 1994), and processed in ArcGIS Pro.

Driftwood Watershed Corn & Soybean Crop Extent, 2021

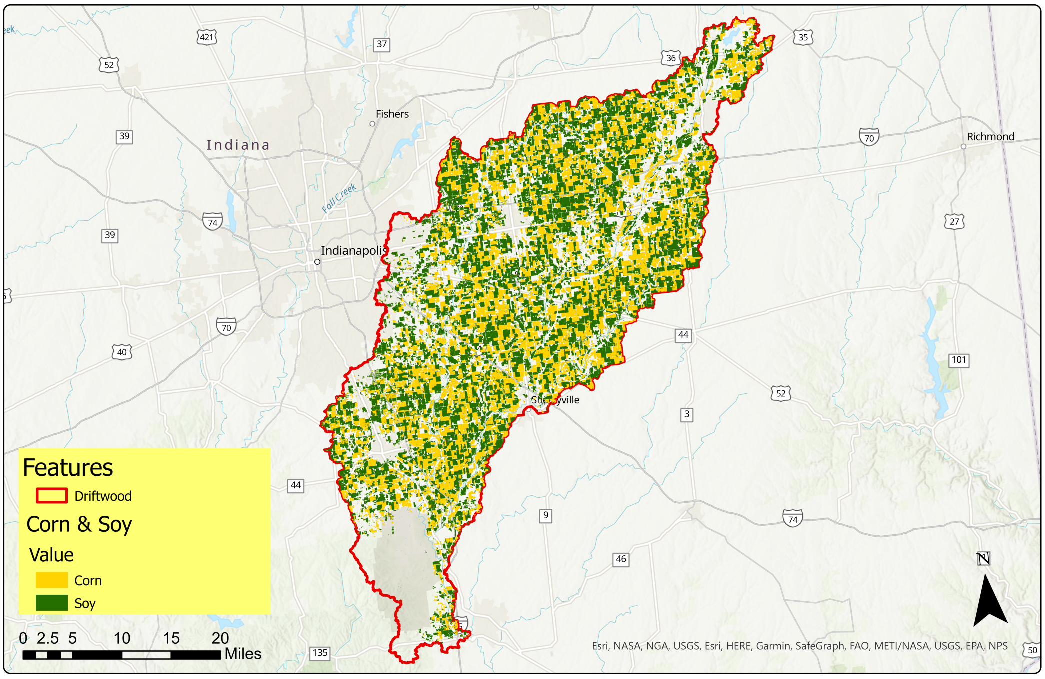

Figure 1: Map of Driftwood watershed boundaries and extent of corn & soybeans in the watershed boundaries.

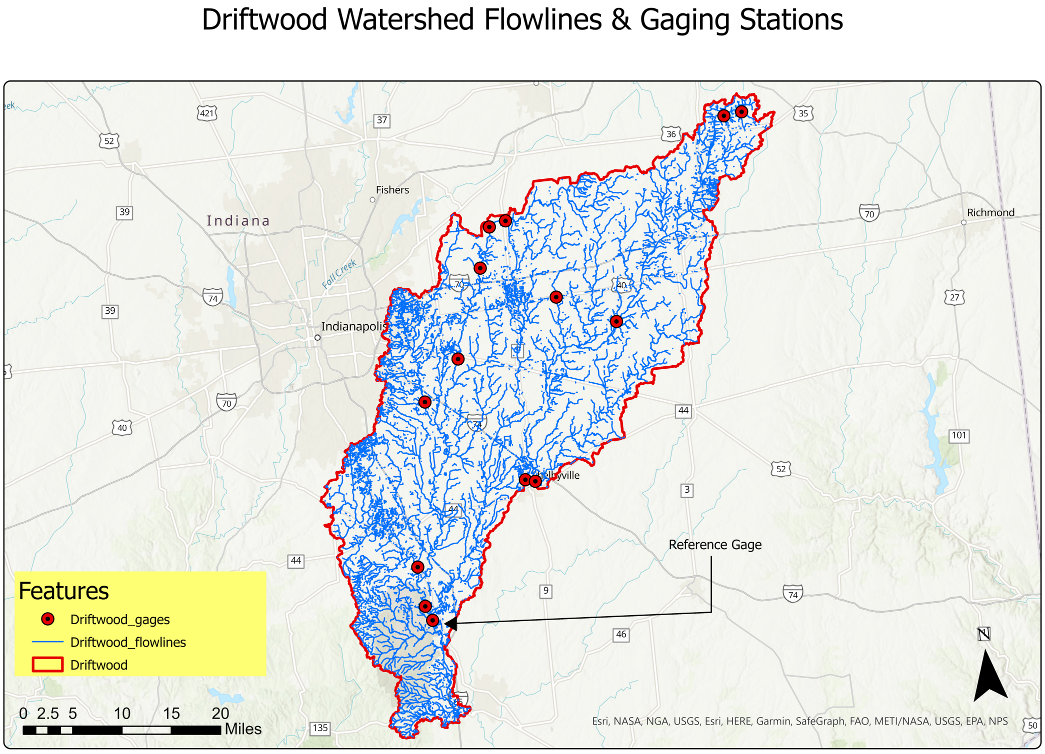

Figure 2: NHD stream flowlines and USGS gaging station locations. Reference gage is indicated by callout arrow.

2.1.1 Hydrologic parameters

Information on flow from the selected USGS gaging station was analyzed to determine a design flow and mass transport rate for the wetland and buffer strip desings. Due to the scale of the Driftwood watershed, flows were evaluated as three-day aggregates, which better models the watershed's likely flow regime. Nitrate transport generally occurs during high flows, with 56% of all nitrate transport occurring during flows $\geq 90^{\text{th}}$ percentile (Royer, David, and Gentry 2006). Flow probabilities were determined quantitatively by ranking three-day aggregated flows and calculating recurrence intervals and probabilities according to equations 1 and 2, where T_r is Recurrence interval, N is the number of years modeled, and M is the rank of the flood in the ranking group, and P is probability (Dingman 2015).

$$T_r = \frac{N+1}{M} \tag{1}$$

$$P = \frac{1}{T_r} \tag{2}$$

The 95^{th} percentile flow in the watershed had a recurrence interval of around 19 three-day periods, corresponding to a two-month return interval, and a design flow of $Q = 846720000$ ft^3 (23976440 m^3) over three days.

2.2 Nutrient Transport

Nutrient loading was estimated based on modeled values of loading and assumptions of mass transport for individual flow events. Data on aggregate N loading were acquired from NOAA's SPARROW model, which estimates total N loading for HUC-8 watersheds (Robertson and Saad 2019). To model a worst-case loading scenario, it was assumed that the total N yield from the watershed was in the form of aquatic NO_3^--N. The SPARROW model estimates that the long-term average annual total N yield for the driftwood watershed is 3181 kg km^{-2} (Robertson and Saad 2019). Referencing this loading to the area of the watershed yields a total mass loading of 9603326 kg N yr^{-1}, following equation 3.

$$\frac{3181.56 \text{ kg}}{\text{km}^2} * 3018.43 \text{ km}^2 = \frac{9603326 \text{ kg N}}{\text{yr}} \tag{3}$$

After determining a total N yield budget for the year, the budget was divided to approximate the total load in each design storm. Assuming on average that an event with a 2-month recurrence interval will happen 6 times a year, and that the design flows transport all 56% of the nutrient transport as found by Royer, David, and Gentry (2006), an individual storm will yield $\frac{56}{6} = 9.333\%$ of the high-flow budget. This corresponds to a mass of 500141.22 kg N per 95^{th} percentile storm, or a concentration of 22.45 mg L^{-1}.

2.3 Constructed Wetland

Constructed wetlands are an enormously complicated and well-studied design topic. To achieve a first-order approximation of the area required for a wetland to reach NO_3^- abatement, the wetland was modeled as a first-order plug flow reactor (PFR) under steady-state conditions (Crites, Middlebrooks, and Reed 2006; Kadlec and Knight 1996; Mines 2014).

2.3.1 Plug flow reaction derivation

The steady-state plug flow reactor equation was derived as follows in equations 4 to 15 (Mines 2014). The basis for all steady state reactions is 4:

$$\text{inputs} - \text{outputs} + \text{reaction} = \text{loss} \tag{4}$$

Substituting transport functions for input, output, and reaction loss functions in equation 4 gives equation 5,

$$\frac{\partial C}{\partial t}\Delta V = QC|_x - QC|_{x+\Delta x} + r\Delta V \tag{5}$$

where ΔV is change in volume, C is concentration, t is time, and r is the reaction loss process in simplified form. Substituting for $QC|_{x+\Delta x}$ and V further gives equation 6:

$$\frac{\partial C}{\partial t}A\Delta x = QC - (QC - (Q\frac{\Delta C}{\Delta x}\Delta x)) + rA\Delta x \tag{6}$$

where A is area and Δx is the distance along the plug flow reactor. Equation 6 simplifies to equation 7:

$$\frac{\partial C}{\partial t} = -(\frac{Q}{A}\frac{\Delta C}{\Delta x}) + r \tag{7}$$

Assuming steady state, concentration is time-invariant and only varies with space. Therefore, $\frac{\partial C}{\partial t} = 0$ and the form of the plug flow equation becomes equation 8:

$$\frac{Q}{A}\frac{\Delta C}{\Delta X} = r \tag{8}$$

A free water surface wetland's NO_3^- removal can be modeled as a first-order plug flow reaction, so that r may be substituted with kC, where k is a first-order reaction constant, yielding equation 9.

$$\frac{Q}{A}\frac{\Delta C}{\Delta x} = -kC \tag{9}$$

Substituting based on equation 10 yields equation 11,

$$\lim_{x\to 0}(\frac{Q}{A}\frac{\Delta C}{\Delta x}) = \frac{Q}{A}\frac{dC}{dx} \tag{10}$$

$$\frac{Q}{A}\frac{dC}{dx} = -kC \tag{11}$$

a first-order, separable ordinary differential equation. To solve for $C(t)$, the derivative is separated, resulting in equation 12:

$$\frac{1}{C}dC = -k\frac{A}{Q}dx \tag{12}$$

and solved by equation 13,

$$\int_{c_0}^{c_t} \frac{1}{C}dC = -k\frac{A}{Q}\int_{x=0}^{x=L} dx \tag{13}$$

yielding equation 14,

$$\ln\frac{c_t}{c_0} = -k\frac{AL}{Q} \tag{14}$$

which rearranges to equation 15,

$$\frac{c_t}{c_0} = e^{-kt} \tag{15}$$

The equation for a plug flow reactor (Mines 2014).

2.3.2 Application to wetland

In equation 15, the ratio of output to input nutrient concentration is determined in the goal-setting process. Limiting effluent to 9 mg L^{-1} would yield an abatement ratio of 0.404 (60.6% abatement). Being temperature-dependent, K is determined through a temperature correction with the Arrhenius equation (Mines 2014; Crites, Middlebrooks, and Reed 2006) as shown in equation 16:

$$k_T = k_{20}(\theta)^{T-20} \tag{16}$$

where $\theta = 1.15$ and $k_{20} = 1.000$ (Crites, Middlebrooks, and Reed 2006).

In the simplest case where $T = 20$°C, the detention time required for a 60.6% abatement is determined by rearranging 15 to solve for t, giving equation 17:

$$t = \frac{\ln \frac{C_t}{C_0}}{-k_{20}} \tag{17}$$

Substituting derived values into equation 17 yields the result in equation 18.

$$t = \frac{\ln 0.404}{-1.000} = 0.91 \text{ days} \tag{18}$$

In addition, surface area can be determined using equation 19 (Crites, Middlebrooks, and Reed 2006):

$$A_s = Q_{avg}\left[\frac{\ln\left(\frac{c_t}{c_0}\right)}{k_t(y)(n)}\right] \tag{19}$$

Where A_s is surface area of the wetland bottom in m^2, y is the depth of water in the wetland in m, and n is the average porosity of the wetland. In this assessment, $y = 0.6$ m and $n = 0.8$, in accordance with literature values (Crites, Middlebrooks, and Reed 2006). Q_{avg} was assumed to be $7.992 * 10^6$ m^3 d^{-1}. In the analysis at 20°C, equation 19 yields the answer in equation 20:

$$7.992 * 10^6 * \left[\frac{\ln(0.404)}{1.000(0.6)(0.8)}\right] = 1.51 * 10^7 \text{m}^2 \tag{20}$$

or 3731 acres. As a size comparison, Goose Pond, a restored wetland near Linton, Indiana, is roughly 9,000 acres (DNR 2021).

2.3.3 Extension to varying temperatures

Equations 17 and 19 depend on k_T and therefore on the temperature at which the reaction occurs, meaning that weather conditions affect the speed and surface area required to process NO_3^-. To simulate the effects of weather, daily temperature and standard deviation data were collected from NOAA NCEI (2022) for Greensburg, IN, and used to create simulated temperature variations in Python.

Temperatures for each day were assumed to be normally distributed independent random variables. One thousand years of randomly simulated data (shown in figure 3) were generated and used to calculate areas and times on a per-day basis. Figure 4 shows the resulting distribution of areas and times required to abate 60.6% of pollution. Days with temperatures $\leq$ 0°C are not shown, as these days are assumed to have no nitrate processing (Crites, Middlebrooks, and Reed 2006). Eighty percent of days required less than 20000 acres of land and 5 days to fully process nitrate. Code used to generate the extension is available in section 6.

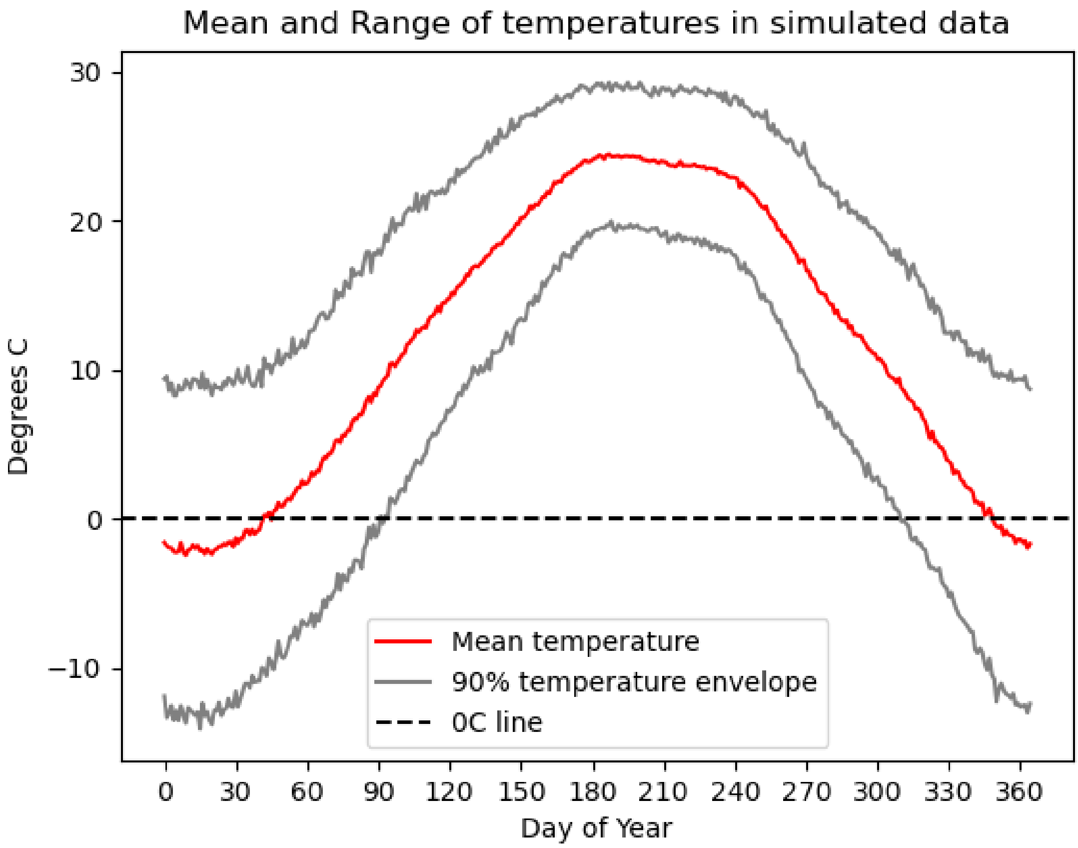

Figure 3: Simulated annual temperature time series, with 90% temperature envelope of random temperatures and 0°C reference line to illustrate proportion of time when temperatures are not conducive to processing of NO_3^-.

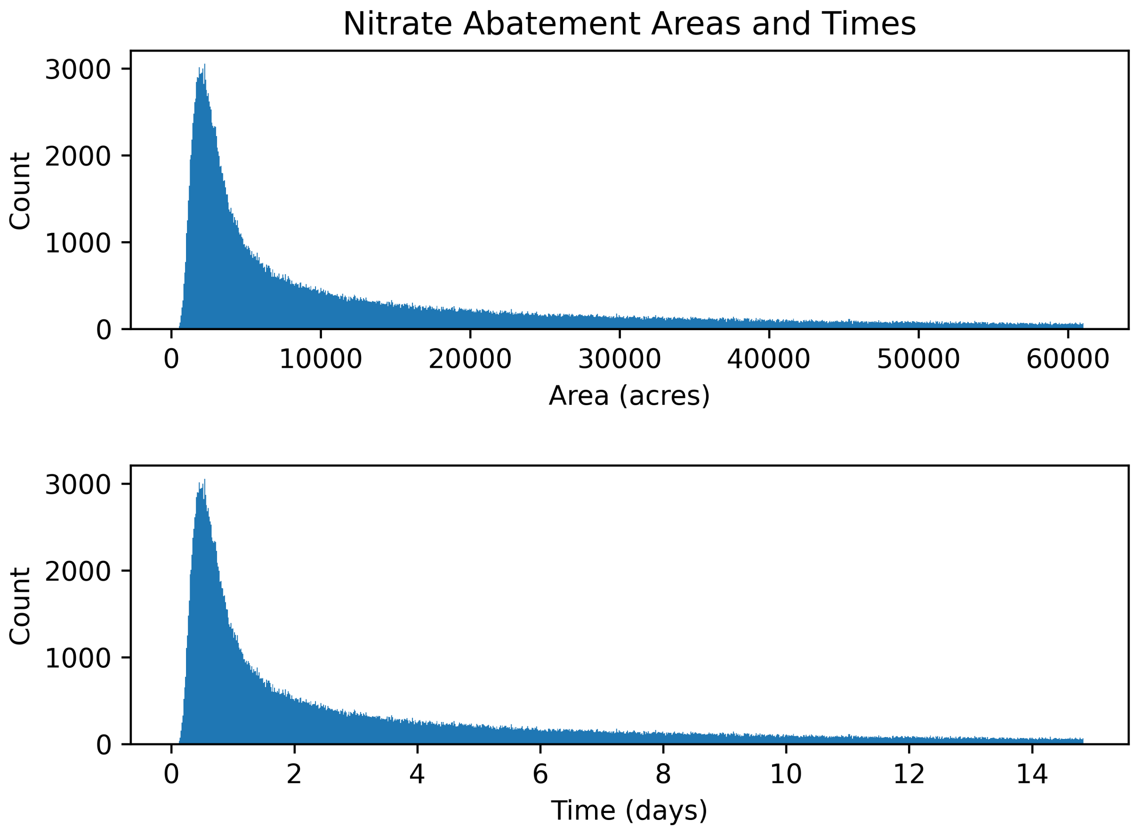

Figure 4: Nitrate abatement times and areas from simulated temperature data, representing a right-skewed distribution of values.

2.4 Buffer Strip

A model for riparian buffer strips was developed from equations for groundwater flow and utilizing existing plug flow equations and values from the constructed wetland literature. Buffer strip denitrification was assumed to occur principally in the reducing subsurface, where it took place with similar reaction constants to a plug flow wetland. Because the model assumes that denitrification only occurs in the subsurface, the buffer strip was treated as a groundwater flow model. The riparian area of the river was divided into buffer sections of length L and a unit width in m. Since the model assumes plug flow, flow is 1-dimensional and there is not lateral mixing of the subsurface flow, meaning that the total processing capacity is the sum of each 1-dimensional slice of the model. Subsurface movement of groundwater is governed by Darcy's law (equation 21), where ϕ is the head and $\frac{d\phi}{dL}$ is the head gradient across the length of the 1-d system; $-K$ is the hydraulic conductivity, and q_x is specific discharge (Haitjema 1995; Bakker and Post 2022). Figure 5 shows a conceptual model of the system (Bakker and Post 2022).

$$q_x = -K\frac{d\phi}{dL} \tag{21}$$

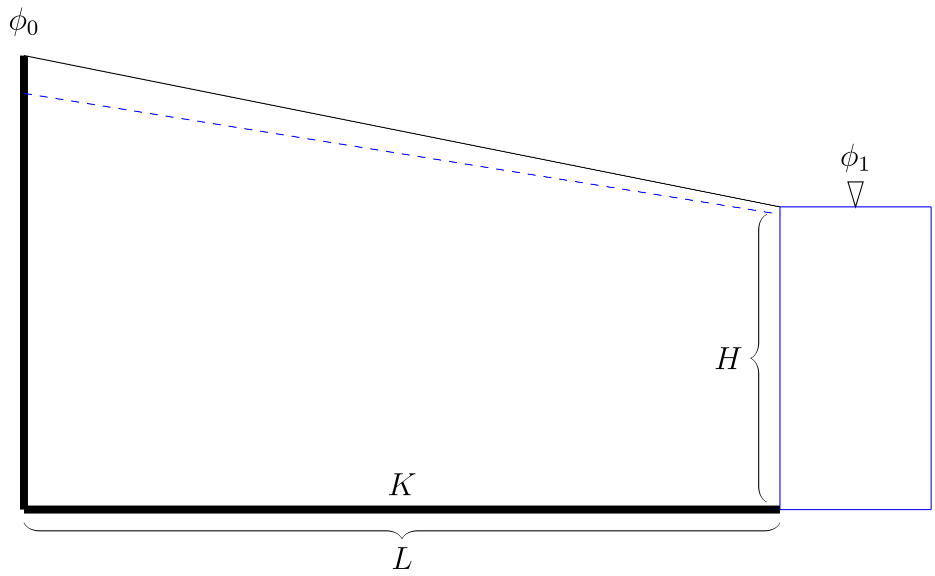

Figure 5: Conceptual 1-d model of groundwater flow system through riparian buffer, after (Bakker and Post 2022).

$\phi|_{x=0}$ is assumed to be fixed at some distance below the subsurface. For the purpose of estimation, it was assumed to be 3m above the set datum. $\phi|_{x=L}$ was assumed to be fixed at 2.134m above datum. Flow was assumed to be unconfined, with a homogeneous isotropic K of 90m d^{-1}.

2.4.1 Length Equation Derivation

To determine the size of the buffer strip, actual velocity of groundwater through the model must be determined. Groundwater velocity is calculated with equation 22:

$$v_x = \frac{q_x}{n_e} \tag{22}$$

where n_e is effective porosity of the substrate (unitless) assumed to be 0.2. Steady-state derivation of equation 21 is along the lines of equations 4 - 17, but without an included reaction (Haitjema 1995). Equations 23 - 27 show the derivation of length from the equation for a plug flow reactor and Darcy's law (Bakker and Post 2022; Haitjema 1995; Dingman 2015). Length may be defined from velocity and time according to equation 23:

$$L = v_x t \tag{23}$$

where L is the length of the buffer strip in m, v_x is the velocity of flow in m d^{-1}, and t is time in days. Equations 17 and 22 are substituted to yield equation 24:

$$L = \left(\frac{q_x}{n_e}\right)\left(\frac{\ln\left(\frac{C_t}{C_0}\right)}{-k_T}\right) \tag{24}$$

Substituting equation 21 into equation 24 gives equations 25 and 26:

$$L = \left(\frac{-K\frac{d\phi}{dL}}{n_e}\right)\left(\frac{\ln\left(\frac{C_e}{C_0}\right)}{-k_T}\right) \tag{25}$$

$$L = \left(\frac{-k(\phi_0 - \phi_1)}{n_e L}\right)\left(\frac{\ln\left(\frac{C_e}{C_0}\right)}{-k_T}\right) \tag{26}$$

Ultimately yielding equation 27:

$$L = \sqrt{\frac{\frac{\ln\left(\frac{C_e}{C_0}\right)}{-k_T}\left(-K\left(\phi_0 - \phi_1\right)\right)}{n_e}} \tag{27}$$

Substituting given values and $k_{T=11.93°\mathrm{C}}$ (annual average temperature) into the equation gives the answer in equation 28:

$$L = \sqrt{\frac{\frac{\ln(0.404)}{0.325}\left(-90\left(3 - 2.134\right)\right)}{0.2}} = 32.97\mathrm{m} \tag{28}$$

Finally, total discharge at the specified L was calculated using equation 29 on a per-slice basis:

$$Q_x = -KH\frac{d\phi}{dL} \tag{29}$$

Resulting in a per-slice discharge of 5.15 $\mathrm{m}^3\ \mathrm{d}^{-1}$. The per-slice discharge value was multiplied by the perimeter of the stream to determine total discharge. Perimeter was derived by buffering flowline streams in the watershed from the National Hydrography Dataset (USGS 2019) in ArcGIS Pro to a width of 1m, yielding a perimeter of 7593237m and a total discharge through the buffer area of 39100224 m^3. Buffering in arcGIS Pro results in a total buffer area of 376934943 m^2 (93143 acres).

2.4.2 Extension to Varying K

As an extension, buffer length was plotted as a function of K throughout a reasonable range of conductivity values. The results are shown in figure 6 and illustrate a log-linear relationship.

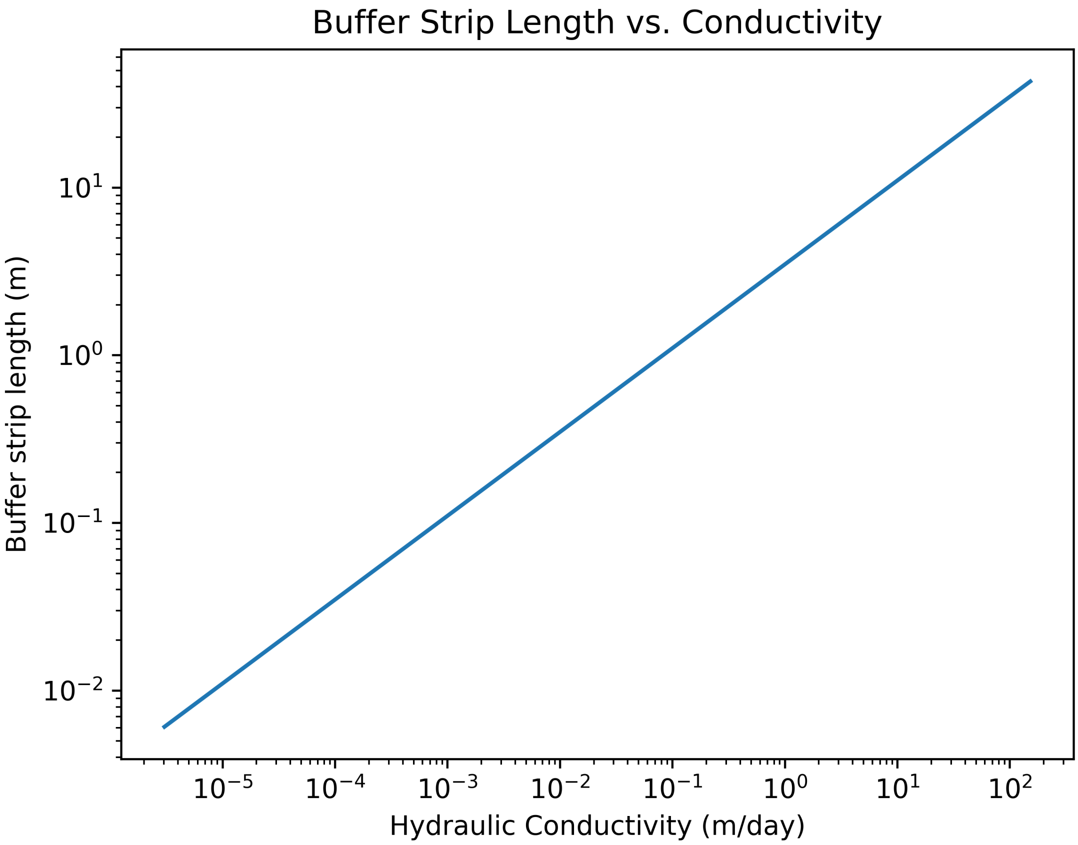

Figure 6: Buffer strip length as a function of K on a log-log scale. The variables have a perfect log-linear relationship under this formulation.

Nearly all conductivities in the simulated range successfully pass the design flow. Figure 7 shows that all values of $k \geq 3.9$ m d^{-1} are sufficient to pass the design flow specification. Full code for this extension may be found in section 6.

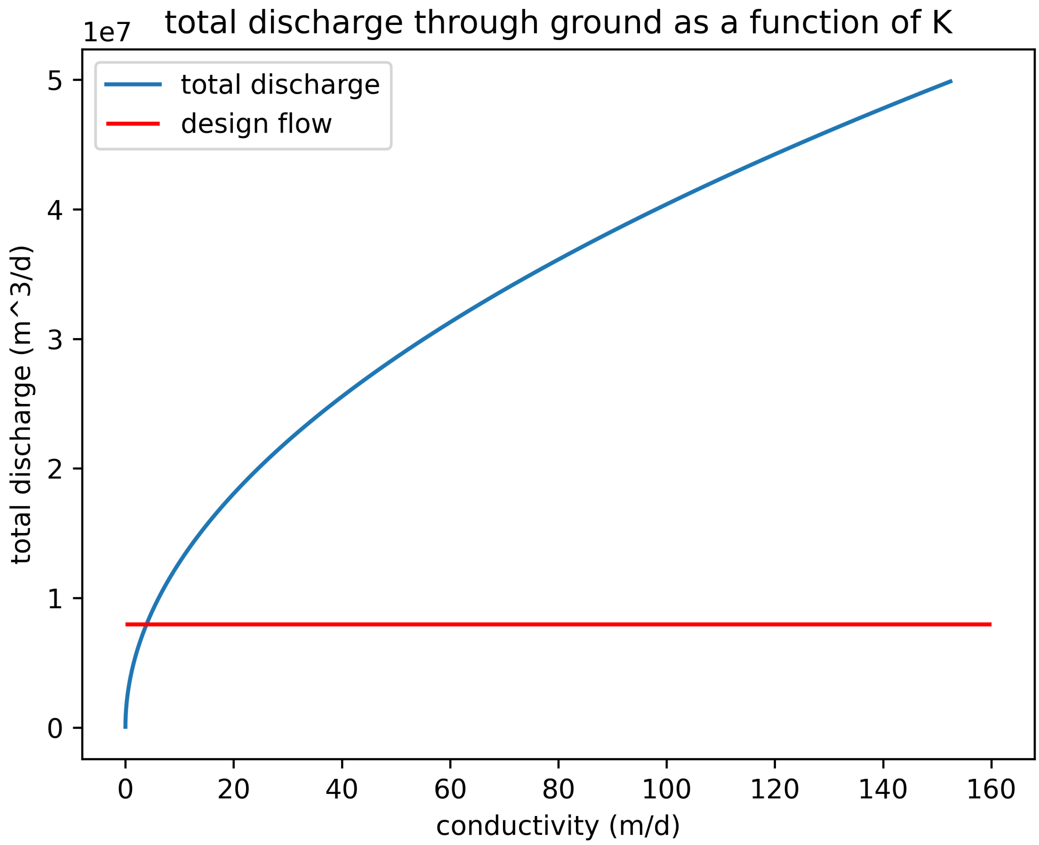

Figure 7: Discharge as a function of conductivity, with a reference line showing the design flow volume.

3 Discussion

Comparing derived area requirements for both models, constructed wetlands seem to be favorable in terms of removal. The wetland required 3731 acres of space at 20°C, and 80% of temperatures completely denitrified with 20000 acres of space, much less than 90000 acres. This finding is partially motivated by differences in reaction temperature, since the subsurface reaction was modeled at 12°C to reflect the fact that subsurface temperatures are generally close to average annual temperature. Assumptions of one-dimensional flow in groundwater also work to grow the estimate for the buffer strip, since an areal model is used instead of a linear model for constructed wetlands, potentially allowing greater surface area and denitrification (Kadlec and Knight 1996; Crites, Middlebrooks, and Reed 2006). One advantage to buffer strips under this specification is that they will work no matter the weather conditions since the subsurface is assumed to be a constant temperature, whereas wetlands have seasonal variations in performance, especially during the winter and spring, when temperatures are highly variable.

Simplifying assumptions made in the hydrologic design parameters and nutrient transport evaluation may substantially change the character of the sizing exercise. Importantly, all nitrogen loadings described in the SPARROW model were assumed to be in the form of nitrate, when in reality different sources give different forms of nitrogen (Kadlec and Knight 1996). The net result was that both models had an overestimated level of annual nitrate loading, potentially by a large factor. While plug flow abatment proceeds similarly irrespective of starting concentration, a larger proportion of nitrate must be abated to meet water quality standards in a higher loading case. Furthermore, nitrate was assumed to be transported in equal proportion during each 95$^{\text{th}}$ percentile storm event, which is very unlikely to be the case. The 95$^{\text{th}}$ percentile storms were assumed to carry all 56% of nitrate that occurred at flows *at or above* the 90$^{\text{th}}$ percentile in Royer, David, and Gentry (2006), potentially biasing the loading estimate even higher.

3.1 Constructed Wetlands

The dynamics of the constructed wetland illustrate a strong temperature-dependence. Figure 4 shows that a high proportion of events would require very little area and time to completely denitrify the effluent stream from a design flow. It logically follows that denitrification would proceed more quickly under warmer conditions. For one, warmer water has less capacity to hold dissolved oxygen (Wetzel, Robert 2001; Raff and Hites 2020). Furthermore, denitrification would proceed faster due to the increased rate bacterial growth in the wetland substrate under higher temperatures (Wetzel, Robert 2001). Climate change will increase average temperatures in Indiana into the 2080s (Widhalm et al. 2018) which means that a higher proportion of days will be warmer, increasing the effectiveness of a constructed wetland. More importantly, rising winter temperatures will reduce the skew of the distribution in figure 4 as winter lows become warmer. More days will also be above freezing, allowing a constructed wetland to denitrify for more of the year as well. This is especially important as many current nutrient export events occur during the winter and spring (Royer, David, and Gentry 2006) and rainfall is projected to intensify through these periods in the future (Widhalm et al. 2018).

The model used to estimate the constructed wetland is limited on several fronts. Importantly, the model is based on a lumped apparent rate constant for denitrification, meaning that only average behaviors are captured in the model (Kadlec and Knight 1996; Crites, Middlebrooks, and Reed 2006). Similarly, steady-state assumptions are a poor fit for the transient nature of nutrient transport. A transient model is substantially more complicated and therefore beyond the scope of present analysis, but is necessary to actually design a wetland system. Furthermore, the only optimization parameter included for comparison is processing size, which ignores political, ecological, logistical, and economic considerations surrounding wetland construction (Crites, Middlebrooks, and Reed 2006; Kadlec and Knight 1996). The wetland was designed under the assumption that nitrate was transported conservatively through the stream network until the point of arrival at the wetland, when in reality it is processed along the length of the stream network to some degree (Wetzel, Robert 2001). While these assumptions alternatively suggest under- and overestimation, the model is most likely underestimating total required area, mostly due to design parameters not factored into the final design, especially a more complicated water budget inside of the wetland itself and more precise biogeochemical estimations (Crites, Middlebrooks, and Reed 2006; Kadlec and

Knight 1996).

3.2 Buffer Strips

The buffer strip model suggests that a relatively small buffer strip could successfully process nitrate in the subsurface flow, and potentially pass the required amount of volume which comprises the storm event. This assumption is reasonably insensitive to K given the results of figure 7. The log-linear relationship between K and length provided in figure 6 is a logical and illustrates the idea that as K decreases, retention time in the soil increases, requiring less buffer length in the ground to achieve the same outcome. For water quality improvement, a 32m buffer is on the high end of size recommendations (Fischer and Fischenich 2000). However, buffer strips which gain other co-benefits such as biodiversity improvement are frequently much wider (Fischer and Fischenich 2000). The relative length of the estimated buffer strip in this analysis is likely due to the limiting assumptions used in modeling.

The buffer strip model is limited in several aspects. By assuming that only groundwater flow mattered for denitrification, plant uptake was completely neglected as a source of nitrogen removal, despite being an important sink for N in most buffer strips (Barling and Moore 1994). This likely increased the size of the buffer strip in the estimation process. Furthermore, variations in topography, subsurface geology, hydrologic conditions and regional groundwater hydrology were ignored, despite being important to the problem (Barling and Moore 1994). The groundwater model is also limited by the assumptions in its boundary conditions, especially the fact that it models the entire length of the stream as gaining and that there is both a constant head and slope down to the river from a certain distance (Dingman 2015). In reality, a transient groundwater model would better describe the dynamics of a rainstorm-driven subsurface flow (Haitjema 1995). Furthermore, the boundary conditions assume there is no flow between the shallow subsurface and deeper groundwater, which would tend to abstract some nitrate to deeper areas or around the stream bed. Streams may also be gaining or losing depending on local hydrological and topographical conditions, further undermining the assumption of uniform riparian conditions (Dingman 2015). The model also assumes full infiltration of the design flow into groundwater, which is unrealistic. Rainfall and infiltration dynamics play an important role in modeling the actual transport of water into the subsurface (Dingman 2015). Subsurface conductivity will also vary depending on location in the watershed, even on a local scale (Bakker and Post 2022; Haitjema 1995), which means that a fixed-width buffer will not work effectively to abate nutrients. Furthermore, the plug flow reactor assumes that the subsurface is sufficiently reducing to remove nitrate, when in reality the subsurface is likely to have an oxidizing layer even in the water table before becoming reducing (Zhang and Furman 2021). Finally, the buffer strips in this model are assumed to be equally effective irrespective of stream order. In reality, buffers strips are most effective on low-order headwater streams (Mander and Tournebize 2015; Stutter, Chardon, and Kronvang 2012). Ultimately, these simplifications suggest that additional modeling, especially regional geology, groundwater flow, and hydrology modeling, should be conducted to improve derived estimates.

4 Recommendations

On the basis of size efficiency, a constructed wetland is the better tool for nutrient abatement in the design watershed. Design size is substantially smaller for the constructed wetland even in relatively cold conditions as compared to riparian buffer strips. However, it is recommended that some combination of buffer strips and a constructed wetland be used in reality. Buffer strips improve riparian habitat and local water quality in a way that a constructed wetland at outflow would not (Stutter, Chardon, and Kronvang 2012; Mander and Tournebize 2015; Barling and Moore 1994). Furthermore, combining approaches will likely improve the size-feasibility of the entire system. Therefore, optimization of both strategies in concert should be a component of further analysis. The buffer strip analysis in particular would also benefit from the inclusion of more variables to better model observed efficiencies in nutrient removal before relying on the model as a decision rule.

5 Conclusion

Nutrient pollution is a critical and ongoing problem for freshwater resources in the United States. Restoration of freshwater ecological features, especially riparian buffers and wetlands, has the potential to substantially reduce nutrient pollution if correctly designed. To support the decision-making process around intervention, evaluation of both alternatives for a case-study watershed was conducted to determine which intervention was most space-efficient. Constructed wetlands were found to be the most space-efficient in the first-approximation evaluation. Further evaluation and modeling should be done to verify the relative areas required for abatement. Wetlands and buffer strips should also be used in conjunction due to the outside benefits each provides.

References

Anbumozhi, Venkatachalam, Jay Radhakrishnan, and Eiji Yamaji. 2005. "Impact of Riparian Buffer Zones on Water Quality and Associated Management Considerations." *Ecological Engineering,* Riparian Buffer Zones in Agricultural Watersheds, 24, no. 5 (May 30, 2005): 517–523. ISSN: 0925-8574, accessed December 4, 2022. https://doi.org/10.1016/j.ecoleng.2004.01.007. https://www.sciencedirect.com/science/article/pii/S092585740500025X.

Bakker, Mark, and Vincent Post. 2022. *Analytical Groundwater Flow Modeling: Theory and Applications Using Python.* First Edition. Boca Raton: Taylor & Francis. ISBN: 978-1-138-02939-2.

Barling, Rowan D., and Ian D. Moore. 1994. "Role of Buffer Strips in Management of Waterway Pollution: A Review." *Environmental Management* 18, no. 4 (July 1, 1994): 543–558. ISSN: 1432-1009, accessed November 16, 2022. https://doi.org/10.1007/BF02400858. https://doi.org/10.1007/BF02400858.

Blann, Kristen L., James L. Anderson, Gary R. Sands, and Bruce Vondracek. 2009. "Effects of Agricultural Drainage on Aquatic Ecosystems: A Review." *Critical Reviews in Environmental Science and Technology* 39, no. 11 (November 2, 2009): 909–1001. ISSN: 1064-3389, 1547-6537, accessed February 14, 2022. https://doi.org/10.1080/10643380801977966. http://www.tandfonline.com/doi/abs/10.1080/10643380801977966.

Bradshaw, Therin M., Abigail G. Blake-Bradshaw, Auriel M. V. Fournier, Joseph D. Lancaster, John O'Connell, Christopher N. Jacques, Michael W. Eichholz, and Heath M. Hagy. 2020. "Marsh Bird Occupancy of Wetlands Managed for Waterfowl in the Midwestern USA." *PLOS ONE* 15, no. 2 (February 21, 2020): e0228980. ISSN: 1932-6203, accessed March 3, 2022. https://doi.org/10.1371/journal.pone.0228980. https://journals.plos.org/plosone/article?id=10.1371/journal.pone.0228980.

Crites, Ronald W., E. Joe Middlebrooks, and Sherwood C. Reed. 2006. *Natural Wastewater Treatment Systems.* First edition. Edited by Michael D. Meyer. Vol. 1. Boca Raton, FL: Taylor & Francis CRC Press. ISBN: 978-0-8493-3804-5.

Dahl, Thomas E. 1990. *Wetlands Losses in the United States, 1780's to 1980's.* U.S. Department of the Interior, Fish and Wildlife Service. Google Books: GhwLAQAAIAAJ.

Dingman, S. Lawrence. 2015. *Physical Hydrology: Third Edition.* 3rd ed. Long Grove, IL: Waveland Press, January 9, 2015. ISBN: 978-1-4786-2807-1. Google Books: rUUaBgAAQBAJ.

DNR, Indiana. 2021. "Goose Pond Fish & Wildlife Area." Indiana Department of Natural Resources, January 29, 2021, 9:38 a.m. (-05:00). Accessed December 2, 2022. https://www.in.gov/dnr/fish-and-wildlife/properties/goose-pond-fwa/.

Doering, Otto C, Francisco Diaz-Hermelo, Crystal Howard, Ralph Heimlich, Fred Hitzhusen, Richard Kazmierczak, John Lee, et al. 1999. "Evaluation of the Economic Costs and Benefits of Methods for Reducing Nutrient Loads to the Gulf of Mexico," 137.

Dudgeon, David, Angela H. Arthington, Mark O. Gessner, Zen-Ichiro Kawabata, Duncan J. Knowler, Christian Lévêque, Robert J. Naiman, et al. 2006. "Freshwater Biodiversity: Importance, Threats, Status and Conservation Challenges." *Biological Reviews* 81 (2): 163–182. ISSN: 1469-185X, accessed November 30, 2022. https://doi.org/10.1017/S1464793105006950. http://onlinelibrary.wiley.com/doi/abs/10.1017/S1464793105006950.

Evenson, Grey R., Heather E. Golden, Jay R. Christensen, Charles R. Lane, Adnan Rajib, Ellen D'Amico, David Tyler Mahoney, Elaheh White, and Qiusheng Wu. 2021. "Wetland Restoration Yields Dynamic Nitrate Responses across the Upper Mississippi River Basin." *Environmental Research Communications* 3, no. 9 (September): 095002. ISSN: 2515-7620, accessed March 4, 2022. https://doi.org/10.1088/2515-7620/ac2125. https://doi.org/10.1088/2515-7620/ac2125.

Fischer, Richard A., and J. C. Fischenich. 2000. *Design Recommendations for Riparian Corridors and Vegetated Buffer Strips.* Technical Note. United States Army Corps of Engineers, April 1, 2000. Accessed October 19, 2022. https://apps.dtic.mil/sti/citations/ADA378426.

Haitjema, Henk M. 1995. *Analytic Element Modeling of Groundwater Flow.* First. Vol. 1. San Diego, California: Academic Press, Inc. ISBN: 0-12-316550-4.

Hammer, Donald, ed. 1989. *Constructed Wetlands for Wastewater Treatment: Municipal, Industrial, and Agricultural.* 1st. Vol. 1. Chelsea, Michigan: Lewis Publishers, Inc. ISBN: 0-87371-184-X.

Hansen, LeRoy, Daneil Hellerstein, Marc Ribaudo, James Williamson, David Nulph, Charles Loesch, and William Crumpton. 2015. "Targeting Investments To Cost Effectively Restore and Protect Wetland Ecosystems: Some Economic Insights," 63.

Hey, Donald L., and Nancy S. Philippi. 1995. "Flood Reduction through Wetland Restoration: The Upper Mississippi River Basin as a Case History." *Restoration Ecology* 3 (1): 4–17. ISSN: 1526-100X, accessed March 1, 2022. https://doi.org/10.1111/j.1526-100X.1995.tb00070.x. http://onlinelibrary.wiley.com/doi/abs/10.1111/j.1526-100X.1995.tb00070.x.

Kadlec, Robert, and Robert Knight. 1996. *Treatment Wetlands.* 1st. 1 vols. Boca Raton, FL: CRC Press, Inc. ISBN: 0-87371-930-1.

Keiser, David A, and Joseph S Shapiro. 2018. "CONSEQUENCES OF THE CLEAN WATER ACT AND THE DEMAND FOR WATER QUALITY," 94.

Kousky, Carolyn, Sheila M. Olmstead, Margaret A. Walls, and Molly Macauley. 2013. "Strategically Placing Green Infrastructure: Cost-Effective Land Conservation in the Floodplain." *Environmental Science & Technology* 47, no. 8 (April 16, 2013): 3563–3570. ISSN: 0013-936X, 1520-5851, accessed March 7, 2022. https://doi.org/10.1021/es303938c. https://pubs.acs.org/doi/10.1021/es303938c.

Kovacic, David A., Mark B. David, Lowell E. Gentry, Karen M. Starks, and Richard A. Cooke. 2000. "Effectiveness of Constructed Wetlands in Reducing Nitrogen and Phosphorus Export from Agricultural Tile Drainage." *Journal of Environmental Quality* 29, no. 4 (July): 1262–1274. ISSN: 0047-2425, 1537-2537, accessed February 25, 2022. https://doi.org/10.2134/jeq2000.00472425002900040033x. https://onlinelibrary.wiley.com/doi/abs/10.2134/jeq2000.00472425002900040033x.

Land, Magnus, Wilhelm Granéli, Anders Grimvall, Carl Christian Hoffmann, William J. Mitsch, Karin S. Tonderski, and Jos T. A. Verhoeven. 2016. "How Effective Are Created or Restored Freshwater Wetlands for Nitrogen and Phosphorus Removal? A Systematic Review." *Environmental Evidence* 5, no. 1 (May 9, 2016): 9. ISSN: 2047-2382, accessed April 26, 2022. https://doi.org/10.1186/s13750-016-0060-0. https://doi.org/10.1186/s13750-016-0060-0.

Mander, Ü., and J. Tournebize. 2015. "Riparian Buffer Zones: Functions and Dimensioning." In *Reference Module in Earth Systems and Environmental Sciences.* Elsevier, January 1, 2015. ISBN: 978-0-12-409548-9, accessed November 20, 2022. https://doi.org/10.1016/B978-0-12-409548-9.09304-0. https://www.sciencedirect.com/science/article/pii/B9780124095489093040.

Mines, Richard O. Jr. 2014. *Environmental Engineering: Principles and Practice.* First. In collaboration with Andre Butler, John C. Little, Zhe Liu, Philip T. McCreanor, John T. Novak, Paige J. Novak, Arthur B. Nunn, and Peter Vikesland. Vol. 1. Chichester, West Sussex, United Kingdom: John Wiley & Sons, Ltd. ISBN: 978-1-118-80145-1.

NCEI, NOAA. 2022. *U.S. Climate Normals Data.* Accessed November 23, 2022. https://www.ncei.noaa.gov/maps/normals/?layers=0000000000001.

Raff, Jonathan, and Ronald Hites. 2020. *Elements of Environmental Chemistry.* 3rd. Vol. 1. Wiley. ISBN: 978-1-119-43487-0.

Reed, Sherwood C., E. Joe Middlebrooks, and Ronald W. Crites. 1988. *Natural Systems for Waste Management & Treatment.* First. Edited by Nadine M. Post and Jim Halston. Vol. 1. United States of America: McGraw-Hill, Inc. ISBN: 0-07-051521-2.

Robertson, Dale M., and David A. Saad. 2019. *Spatially Referenced Models of Streamflow and Nitrogen, Phosphorus, and Suspended-Sediment Loads in Streams of the Midwestern United States.* USGS Numbered Series, Scientific Investigations Report 2019-5114. Reston, VA: U.S. Geological Survey. Accessed November 30, 2022. https://doi.org/10.3133/sir20195114. http://pubs.er.usgs.gov/publication/sir20195114.

Royer, Todd V., Mark B. David, and Lowell E. Gentry. 2006. "Timing of Riverine Export of Nitrate and Phosphorus from Agricultural Watersheds in Illinois: Implications for Reducing Nutrient Loading to the Mississippi River." *Environmental Science & Technology* 40, no. 13 (July 1, 2006): 4126–4131. ISSN: 0013-936X, 1520-5851, accessed March 4, 2022. https://doi.org/10.1021/es052573n. https://pubs.acs.org/doi/10.1021/es052573n.

Segerson, Kathleen, and Dan Walker. 2002. "Nutrient Pollution: An Economic Perspective." *Estuaries* 25, no. 4 (August): 797–808. ISSN: 0160-8347, accessed October 27, 2022. https://doi.org/10.1007/BF02804906. http://link.springer.com/10.1007/BF02804906.

Shortle, James, and Richard D. Horan. 2017. "Nutrient Pollution: A Wicked Challenge for Economic Instruments." *Water Economics and Policy* 03, no. 02 (April 1, 2017): 1650033. ISSN: 2382-624X, accessed October 17, 2021. https://doi.org/10.1142/S2382624X16500338. http://www.worldscientific.com/doi/abs/10.1142/S2382624X16500338.

Stutter, Marc I., Wim J. Chardon, and Brian Kronvang. 2012. "Riparian Buffer Strips as a Multifunctional Management Tool in Agricultural Landscapes: Introduction." *Journal of Environmental Quality* 41 (2): 297–303. ISSN: 1537-2537, accessed December 4, 2022. https://doi.org/10.2134/jeq2011.0439. https://onlinelibrary.wiley.com/doi/abs/10.2134/jeq2011.0439.

USDA. 2021. *2021 USDA Cropland Data Layer.*

USGS. 1994. "USGS Water Data for the Nation," accessed December 7, 2022. https://doi.org/10.5066/F7P55KJN. https://waterdata.usgs.gov/nwis.

———. 2019. *National Hydrography Dataset (NHDPlus HR).* Accessed November 20, 2022. https://www.usgs.gov/national-hydrography/access-national-hydrography-products.

Ward, Mary H., Rena R. Jones, Jean D. Brender, Theo M. de Kok, Peter J. Weyer, Bernard T. Nolan, Cristina M. Villanueva, and Simone G. van Breda. 2018. "Drinking Water Nitrate and Human Health: An Updated Review." *International Journal of Environmental Research and Public Health* 15, no. 7 (July): 1557. ISSN: 1661-7827, accessed March 4, 2022. https://doi.org/10.3390/ijerph15071557. pmid: 30041450. https://www.ncbi.nlm.nih.gov/pmc/articles/PMC6068531/.

Wetzel, Robert. 2001. *Limnology.* 3rd. 525 B. Street, Suite 1900, San Diego, California: Elsevier. ISBN: 978-0-12-744760-5.

Widhalm, Melissa, Alan Hamlet, Kyuhyun Byun, Scott Robeson, Mike Baldwin, Paul Staten, Chun-mei Chiu, et al. 2018. "Indiana's Past & Future Climate: A Report from the Indiana Climate Change Impacts Assessment." *Climate Change Reports* (March 1, 2018). https://doi.org/10.5703/1288284316634. https://docs.lib.purdue.edu/climatetr/2.

Wine, Michael L., and Jason H. Davison. 2019. "Untangling Global Change Impacts on Hydrological Processes: Resisting Climatization." *Hydrological Processes* 33 (15): 2148–2155. ISSN: 1099-1085, accessed February 8, 2022. https://doi.org/10.1002/hyp.13483. http://onlinelibrary.wiley.com/doi/abs/10.1002/hyp.13483.

Yang, Guoxiang, and Elly P. H. Best. 2015. "Spatial Optimization of Watershed Management Practices for Nitrogen Load Reduction Using a Modeling-Optimization Framework." *Journal of Environmental Management* 161 (September 15, 2015): 252–260. ISSN: 0301-4797, accessed February 26, 2022. https://doi.org/10.1016/j.jenvman.2015.06.052. https://www.sciencedirect.com/science/article/pii/S0301479715301444.

Zhang, Zengyu, and Alex Furman. 2021. "Soil Redox Dynamics under Dynamic Hydrologic Regimes - A Review." *Science of The Total Environment* 763 (April 1, 2021): 143026. ISSN: 0048-9697, accessed December 7, 2022. https://doi.org/10.1016/j.scitotenv.2020.143026. https://www.sciencedirect.com/science/article/pii/S0048969720365566.

6 Appendix: Code

```
import pandas as pd
import scipy as sp
import numpy as np
import matplotlib.pyplot as plt
import matplotlib.dates
import math

#getting some basic hydrology information from the watershed:

flow = pd.read_csv("F:/Home/School Files/University files/Grad School/S2 2022/Environmental \
Engineering/Project_Data/Flow_Data_USGS_03363000.txt", delimiter='\s+')

#getting datetimes & indexing.
flow['datetime'] = pd.to_datetime(flow['datetime'])
flow.set_index(keys= flow['datetime'], inplace=True)

#slicing the last 5 water years
#for some information on typical recent patterns:

flow_wy1722 = \
flow[(flow['datetime'] > '2017-09-30') & (flow['datetime'] < '2022-10-01')]
flow_wy1722['vol_passed'] = flow_wy1722['mdcfs'] * 60 * 60 * 24
flow_wy1722.dropna(inplace=True)

#Getting a measure of accumulated flow
flow_wy1722['flow_accum_percent'] = ((flow_wy1722['vol_passed'].cumsum() / \ sum(flow_wy1722['vol_pa

plt.plot(flow_wy1722['datetime'], flow_wy1722['flow_accum_percent'])
plt.axvline(x= flow_wy1722['datetime'].loc['2018-10-01'],ymin=0, ymax=101, color='r')
plt.axvline(x= flow_wy1722['datetime'].loc['2019-10-01'],ymin=0, ymax=101, color='r')
plt.axvline(x= flow_wy1722['datetime'].loc['2020-10-01'],ymin=0, ymax=101, color='r')
plt.axvline(x= flow_wy1722['datetime'].loc['2021-10-01'],ymin=0, ymax=101, color='r')
plt.grid(True)
plt.show()

#More formal information on peak flows:

#first get a slice of time with consistent land use patterns;

flow_8021 = flow[(flow['datetime'] >= '1980-01-01') & (flow['datetime'] <= '2021-12-31')]


#next sort the events by size and pull the first one from each year:

#integrating the rate to get a total volume passed in a day:
flow_8021['vol_passed'] = flow_8021['mdcfs'] * 60 * 60 * 24
flow_8021.dropna(inplace=True)
flow_8021['year'] = flow_8021['datetime'].dt.year
flow_8021_group = flow_8021.groupby(['year'])['vol_passed'].max()
flow_sorted_8021 = flow_8021_group.sort_values(ascending=False)
```

```
ranks = np.arange(1,(len(flow_sorted_8021)+1), step=1)
flow_sorted_ranked_8021 = flow_sorted_8021.to_frame()
flow_sorted_ranked_8021['rank'] = np.arange(1,(len(flow_sorted_8021)+1),step=1)
flow_sorted_ranked_8021['RI'] = (24/(flow_sorted_ranked_8021['rank']))
flow_sorted_ranked_8021['prob'] = (1/flow_sorted_ranked_8021['RI'])


flow_3d= flow_8021.resample("3d", label="left").sum()
flow_sorted_3d = flow_3d.sort_values(['vol_passed'], ascending=False)
flow_sorted_3d['rank'] = np.arange(1,(len(flow_sorted_3d)+1),step=1)
flow_sorted_3d['year'] = flow_sorted_3d.index.year
flow_sorted_3d['RI'] = ((len(flow_sorted_3d)+1)/(flow_sorted_3d['rank']))
flow_sorted_3d['prob'] = (1/flow_sorted_3d['RI'])


design_3d_flows = flow_sorted_3d[(flow_sorted_3d['RI']<130) & (flow_sorted_3d['RI']> 110)]

design_3d_flows['vol_passed'].mean()

flow_sorted_3d[(flow_sorted_3d['prob']<=0.11) & (flow_sorted_3d['prob']>=0.05)]


#getting flow percentiles to be more accurate with our streamflow measurement

## let's build a model to simulate a once-every-2mos flow
# and how it changes the area requirements and processing time/precision.

#start by getting some average temperature information for the driftwood watershed:
#long-term mean  temp for each day in the year:

climdat = pd.read_csv("C:/Users/brown/Downloads/3140615.csv")

temps = climdat[['DLY-TAVG-NORMAL', 'DLY-TAVG-STDDEV']]

#Now I need to generate a synthetic dataset which allows for some stochastic modeling.

#Step 1: use the long-term daily averages and standard deviations
#to generate synthetic temp data for a large number of 'years'.

rows = 365
cols = 100
simulated_data = pd.DataFrame()

def f_to_c(temp_f):
    temp_c = (temp_f - 32)*(5/9)
    return(temp_c)

#generating synthetic temperature data from mean & sd for each data:

simulated_data = pd.DataFrame()
for i in range(0,len(temps)):
    samples = np.random.normal(temps.loc[i][0], temps.loc[i][1], 1000)
```

```
    simulated_data[f'day{i}'] = pd.Series(samples)

sim_dat_ts = simulated_data.transpose() #transposing

simdat_c = f_to_c(sim_dat_ts) #converting the temps to Celsius

#summary plot of the temperature data to help with visualization:

plt.plot(simdat_c.transpose().mean(), color='red', label="Mean temperature") #mean
plt.plot(simdat_c.transpose().quantile(0.95), color='gray', label="90% temperature envelope")
plt.plot(simdat_c.transpose().quantile(0.05), color='gray') #5th percentile (lows)
plt.axhline(y=0, color='black', linestyle='--', label='0C line') #0c line
plt.xticks(ticks = np.arange(0,365, 30), labels=np.arange(0,365, 30)) #fixing xticks
plt.xlabel("Day of Year")
plt.ylabel("Degrees C")
plt.title("Mean and Range of temperatures in simulated data")
plt.legend()
plt.savefig("Temp_Sim_Dist.png", resolution= 300)
plt.show()



k20amm = 0.2187 #constants to correct temp for nitrate, ammonia
k20nit = 1.000

constsamm = k20amm * ((1.048)**(simdat_c - 20)) #arrhenius adjustments
constsamm[constsamm <= k20amm * ((1.048)**(0-20))] = 0

constsnit = k20nit * ((1.15)**(simdat_c - 20))
constsnit[constsnit <= k20nit * ((1.15)**(0-20))] = 0


#next we're going to calculate times for our abatement goals based on these constants

# t = (ln(ce/c0)/kt)

#ammonia - 50% abatement

timesamm = (np.log(0.5)/-constsamm)
timesamm[timesamm > 1000000000000000000000000000000000000] = np.nan

#nitrate = 60% abatement
timesnit = (np.log(0.404)/-constsnit)
timesnit[timesnit > 1000000000000000000000000000000000000] = np.nan
#areas:
#A_s = Q_a [ (ln(c_0/c_e)) / K_t*y*n ] y and n are constants. n = 0.8 and y = 0.6m

n = 0.8
y = 0.6
Q_a = 7992000 #Design flow in cubic meters per day.

areasamm = (Q_a*((np.log(0.5)) / (-constsamm * y * n)))

areasamm[areasamm > 1000000000000000000000000000000] = np.nan
```

```
areasnit = (Q_a*((np.log(0.404)) / (-constsnit * y * n)))
areasnit[areasnit > 100000000000000000000000000000] = np.nan

acresamm = areasamm / 4046.86
acresnit = areasnit / 4046.86

plt.subplot(2,2,1)
plt.hist(areasamm.to_numpy().flatten(), bins=100)
plt.subplot(2,2,3)
plt.hist(areasnit.to_numpy().flatten(), bins=100)
plt.show()

#average of 58 days a year where it is too cold for the wetland to function (<= 0 degrees C)


fig, axs = plt.subplots(nrows= 2, ncols=2, sharey=True)
axs[0,0].hist(acresamm.to_numpy().flatten(), bins=1000)
axs[0,0].set_title('Ammonia Abatement Area Histogram')
axs[0,0].set(xlabel = 'Area (ac)', ylabel='Count')
axs[1,0].hist(acresnit.to_numpy().flatten(), bins=1000)
axs[1,0].set_title('Nitrate Abatement Area Histogram')
axs[1,0].set(xlabel='Area (ac)', ylabel='Count')
axs[0,1].hist(timesamm.to_numpy().flatten(), bins=1000)
axs[0,1].set_title('Ammonia Abatement Time Histogram')
axs[0,1].set(xlabel='Time (days)', ylabel = "Count")
axs[1,1].hist(timesnit.to_numpy().flatten(), bins=1000)
axs[1,1].set_title('Nitrate Abatement Time Histogram')
axs[1,1].set(xlabel = "Time (days)", ylabel="Count")
fig.tight_layout(pad=2)
plt.show()

plt.subplot(2,1,1)
plt.hist(((areasnit.to_numpy().flatten())/4046.86), bins=1000)
plt.xlabel("Area (acres)")
plt.ylabel("Count")
plt.tight_layout(pad=2)
plt.title("Nitrate Abatement Areas and Times")
plt.subplot(2,1,2)
plt.hist(timesnit.to_numpy().flatten(),bins=1000)
plt.xlabel("Time (days)")
plt.ylabel("Count")
plt.tight_layout(pad=2)
plt.savefig("Nitrate_Abatement_distribution.png", dpi=600)
plt.show()

flat_acres = acresnit.to_numpy().flatten()
filter_arr = []

for elem in flat_acres:
    if elem >= 20000:
        filter_arr.append(True)
    else:
        filter_arr.append(False)
```

```python

flat_extreme = flat_acres[filter_arr]
len(flat_extreme)

print(len(flat_extreme)/len(flat_acres) * 100)

flat_times = timesnit.to_numpy().flatten()
filter_arr = []

for elem in flat_times:
    if elem >= 5:
        filter_arr.append(True)
    else:
        filter_arr.append(False)

flat_time_extreme = flat_times[filter_arr]
len(flat_time_extreme)

print(len(flat_time_extreme)/len(flat_times) * 100)

#groundwater extension: what about different values of K?

#first get a vector of ks in meters:

def ft_to_m(ft):
    m = ft/3.28
    return m


conds_m = np.arange(ft_to_m(0.001), ft_to_m(500), step=ft_to_m(0.001))

#now we write the equation to send them all through:

gw_lengths = (((np.log(0.404)/-0.325)*((conds_m)*(3-2.134))) /0.2)**0.5

#plotting
plt.plot(conds_m, gw_lengths)
plt.xlabel('Hydraulic Conductivity (m/day)')
plt.ylabel('Buffer strip length (m)')
plt.title("Buffer Strip Length vs. Conductivity")
plt.loglog()
plt.savefig("Buffer_Strip_func_K", dpi=600)
plt.show()

#let's find the discharge through the perimeter area

#from the GIS analysis of perimeter:
perimeter_stream = 7593236.851623

#the Q_x function:

total_discharge = (90*2.134*perimeter_stream*perimeter_stream)*((3-2.134)/32.30)

design_flow = 23976440.3464/3
```

```
total_discharge/design_flow

#it's 4 times the magnitude.

total_disch_vect = (conds_m*2.134*perimeter_stream)*((3-2.134)/gw_lengths)

plt.plot(conds_m, total_disch_vect, label="total discharge")
plt.hlines(y=design_flow, xmin=0, xmax=160, color='r', label="design flow")
plt.xlabel('conductivity (m/d)')
plt.ylabel('total discharge (m^3/d)')
plt.title('total discharge through ground as a function of K')
plt.legend(loc = 0)
#plt.savefig("Q_vs_Cond", dpi=600)
plt.show()
```